

Fabrication of Microcavity Mirrors for high precision Sensing of a Levitated Nanosphere

Semester Thesis

Author:

Dominik Werner

Supervisors:

Dr. René Reimann

Dominik Windey

Prof. Dr. Lukas Novotny

Photonics Laboratory
Swiss Federal Institute of Technology Zurich

December 2018

Abstract

For exploring the boundaries between the micro- and the macroscopic world we work with mesoscopic glass particles. A nano-scale glass particle can be detached from most environmental influences by putting it into a vacuum and using a laser beam to levitate it. The suspension of the particle does not rely on radiation pressure but on the gradient force which is dominant at this scale. To have a high quality factor it is important to have a high signal-to-noise ratio. This can be achieved by using a cooling mechanism to account for the forces exerted on the particle by residual gas molecules. The cooling which is done by moving the trapping beam with a piezo-stage needs a feedback loop in order to work properly with an accurate measurement of the particles current location. One way to measure the particles position is by adding an optical cavity around the particle which will cause the scattered light to form a mode inside of it. Part of the mode will be coupled out of the cavity and can be used to determine the position of the particle via the measured intensity. To improve this method this semester thesis has the goal of finding a feasible method for fabricating a microcavity. Microcavities have a much smaller mode volume which leads to the particles presence having a much bigger impact on the measured intensity at the detector outside of the cavity.

Contents

1	Introduction	1
2	Theory	3
2.1	Laser trapping	3
2.2	Feedback Cooling	5
2.3	Cavity particle detection	5
2.4	Figures of merit	6
2.4.1	Sensing factor	6
2.4.2	Information retrieval rate	6
2.4.3	Detection efficiency	6
3	Fabrication	7
3.1	Requirements	7
3.1.1	Cavity Length	7
3.1.2	Wavefront radius	9
3.1.3	Surface roughness	9
3.2	Process	11
3.2.1	Overview	11
3.2.2	Cleaning	11
3.2.3	Stamp fabrication	11
3.2.4	Measurement	14
3.2.5	Silanization	16
3.2.6	Coverslip preparation	17
3.2.7	Mirror imprinting	17
3.2.8	Grinding	17
3.2.9	Cleaning	17
3.2.10	Coating	17
3.3	Process Evaluation	18
3.4	Analysis	18
4	Results	19
5	Summary and Outlook	21

1 Introduction

For the purpose of sensing very tiny masses, charges, magnetic fields or weak forces, recent developments in optomechanics have brought forth resonators with very high Q-factors which are potentially capable doing such measurements. Limitation of such resonators are that they are susceptible to temperature fluctuations, dissipation losses as well as thermomechanical noise. To omit those kinds of problems a different kind of resonator can be used, a levitated nanoparticle in high vacuum [nphys2798.pdf]. Such a particle can achieve a very high Q-factor that is only limited by the collision with residual air molecules. In order for the levitated nanoparticle to act as a resonator with high Q-factor the influence of thermal noise has to be mitigated by using feedback cooling. It has been shown that a very promising way of measuring the required parameters for said feedback cooling is the placement of the nanoparticle in an optical cavity which couples out the light of the cavity mode, generated by scattered light, hereby allowing to very precisely determine the influence of the nanoparticle on the light.

The goal of this work is to further improve the feedback cooling mechanism by developing a feasible method to fabricate microcavities for the nanoparticle to be put inside of. The advantage of very small cavities compared to larger ones is that the difference of the mode volume inside of the cavity is smaller than before which gives the presence of the the very small nanoparticle more significance in terms of the impact of the cavity linewidth compared to a larger cavity. With this new cavity fabrication method we hope to optimize the feedback cooling mechanism by being able to determine the exact state of the particle inside of the cavity more accurately. Ultimately the goal is to use the knowledge of past setups that used larger cavities and build a new setup that allows the full exploration of the possibilities that this new configuration enables us to do.

2 Theory

The aim of this chapter is to offer a brief introduction into the basics of the trapping experiment and the cavity theory necessary to discuss the fabrication process of the microcavity mirrors. It will by no means offer a complete picture nor a formal derivation of the physics involved in the trapping of a nanosphere, but will highlight the important results made in more rigorous works concerned with the topic.

2.1 Laser trapping

At the heart of the experiment which we want to improve with the fabrication of microcavity mirrors is the levitated nanosphere which is made from siliciumdioxid. The trapping of the nanoparticle is achieved with a highly focused laser beam which effectively traps the particle. We speak of cooling because the motion of the particle is reduced by its isolation from the environment. If trapped in vacuum only residual air molecules will collide with the particle causing a certain randomness to its oscillating movement.

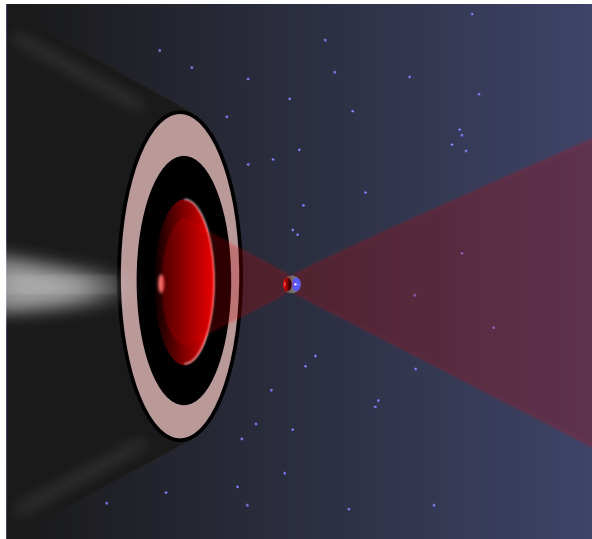


Figure 2.1: A glass nanoparticle is trapped by a strongly focused laser beam. Residual air molecules collide with the particle which gives rise to small force. (based on an illustration found in [ref])

The question is, how can the tightly focused laser beam trap the nanoparticle? To answer this question we have to use an appropriate physical description of the situation at hand. The size of the particle is approximately 150 nm. Because the particle is so small ($2r \ll \lambda$) we may treat it as a dipole with polarizability $\alpha = \alpha' + i\alpha''$. This is

2 Theory

very useful since for determining the optical forces which are at play here we need to know the full description of the electric and magnetic fields. We further assume that our laser is a monochromatic source of a single wavelength λ . In this case the time-averaged optical force is which acts on the particle at position $\mathbf{r} = (r_x, r_y, r_z)^T$ only depends on the incident field [ref].

$$\langle \mathbf{F}_{\text{opt}} \rangle(\mathbf{r}) = \frac{\alpha'}{2} \sum_i \operatorname{Re} \{ E_i^*(\mathbf{r}) \nabla E_i(\mathbf{r}) \} + \frac{\alpha''}{2} \sum_i \operatorname{Im} \{ E_i^*(\mathbf{r}) \nabla E_i(\mathbf{r}) \} , i \in \{x, y, z\} \quad (2.1)$$

The electric field in the equation stated above refers to the complex electric field which defines the time-dependent, real field.

$$\mathbf{E}_i(\mathbf{r}, t) = \operatorname{Re} \{ \mathbf{E}_i(\mathbf{r}) e^{-i\omega t} \} \quad (2.2)$$

Where the angular frequency is defined as $\omega = 2\pi c_0/\lambda$. The first part of Equation 2.2 can be rewritten, such that it becomes obvious why this term is called the *gradient force*.

$$\langle \mathbf{F}_{\text{grad}} \rangle(\mathbf{r}) = \frac{\alpha'}{4} \nabla (\mathbf{E}_i(\mathbf{R}) \cdot \mathbf{E}_i^*(\mathbf{r})) = \frac{\alpha'}{2c_0 \varepsilon_0} \nabla I(\mathbf{r}) \quad (2.3)$$

This force scales with the gradient of the electric field intensity $I(\mathbf{r})$. The particles used in the experiment all have a polarizability with positive real part which means that they are attracted to intensity maxima. The formal treatment of the second term in Equation 2.2 does not yield itself to the same transformation. It is called the *scattering force*.

$$\langle \mathbf{F}_{\text{scat}} \rangle(\mathbf{r}) = \frac{\alpha''}{\omega} \mu_0 \langle \mathbf{S} \rangle(\mathbf{r}) - i \frac{\alpha''}{4} [\nabla \times (\mathbf{E}_i(\mathbf{r}) \times \mathbf{E}_i(\mathbf{r}))] \quad (2.4)$$

While the gradient force is conservative ($\nabla \times \langle \mathbf{F}_{\text{grad}} \rangle = 0$) and does not do any work on the particle the same cannot be said about the scattering force. The first term in Equation 2.4 points in the direction of the *time averaged pointing vector* $\langle \mathbf{S} \rangle$ which means the force pushes in the direction of the power flux. The second term has to do with the spin density of the light field [maybe ref again].

The electrostatic polarizability of a spherical particle with permittivity ε_p and radius a , surrounded by a material of permittivity ε_m is given by [ref]:

$$\alpha_p(\omega) = 4\varepsilon_0 \pi a^3 \frac{\varepsilon_p(\omega) - \varepsilon_m(\omega)}{\varepsilon_p(\omega) + 2\varepsilon_m(\omega)} \quad (2.5)$$

In our case the particle is situated in vacuum which leads to $\varepsilon_m = 1$. Since ε_m in general can be absorptive and have an imaginary part we ought to apply a correction to the polarizability [ref].

$$\alpha(\omega) = \frac{\alpha_p(\omega)}{1 - i \frac{k^3}{6\pi\varepsilon_0} \alpha_p(\omega)} \approx \alpha_p(\omega) + i \frac{k^3}{6\pi\varepsilon_0} \alpha_p^2(\omega) \quad (2.6)$$

This defines $\alpha' = \alpha_p$ and $\alpha'' = k^3/(6\pi\varepsilon_0)\alpha'^2$. From this we can see that the gradient force scales linearly with the particle volume $V = 4/3\pi a^3$ and the scattering force with V^2 . This means the gradient force is dominant for nanosized particles and that trapping

requires no additional cooling.

To illustrate how the optical forces can trap the particle, we have plotted the field intensities and the forces along the three axis in [autoref]. For this calculation a Gaussian beam was chosen even tough quantitatively speaking this is not correct. Since we have a tightly focused beam this model is not sufficient. On the other hand, qualitatively speaking this simple model illustrates nicely the effect that also occurs in other models which are more suitable for a tightly focused beam [ref]. (calculate the gradient force and field intensities in x, y, z maybe use complex origin fields)

2.2 Feedback Cooling

Once the particle is trapped inside the beam it oscillates with a resonance frequency Ω_p around the focus point. The equation of motion can be defined as:

$$m\ddot{\mathbf{r}}(t) + m\gamma\dot{\mathbf{r}}(t) + \mathbf{F}_{\text{grad}}(t) = \mathbf{F}_{\text{fluct}}(t) + \mathbf{F}_{\text{scat}}(t) + \sum \mathbf{F} \quad (2.7)$$

Since there are still air molecules around the particle we have a damping with damping rate γ . $\mathbf{F}_{\text{fluct}}$ is the total fluctuating force. The last term represents all the additional forces that may act on the particle. From this equation the resonance frequency Ω_p of the particle can be extracted.

With the knowledge about the particles movement the cooling aims at cancelling it. This means that once the particle moves away from a defined center point, the feedback mechanism tells the setup to readjust. Since the oscillations of the particle are taking place in the nanometer regime, this can be implemented by moving the trapping laser with a piezo-stage [ref].

2.3 Cavity particle detection

Previously we discussed how a feedback mechanism can be used to account for sudden displacements of the particle. There exist different methods how to detect the particles position and motion. This work focuses on a mechanism that uses an optical cavity to acquire information about the particles location and movement.

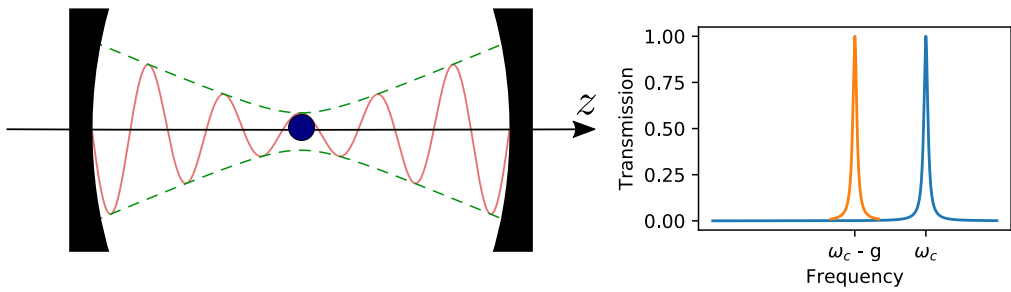


Figure 2.2: •

2.4 Figures of merit

2.4.1 Sensing factor

$$S \propto \frac{\mathcal{F}}{L} \quad (2.8)$$

2.4.2 Information retrieval rate

2.4.3 Detection efficiency

3 Fabrication

3.1 Requirements

The main aim of this project is to establish a fabrication process for microcavity mirrors of medium-high finesse. As the microcavity will be implemented in a particle trapping experiment it is essential to ensure geometrical compatibility between cavity and particle trap.

3.1.1 Cavity Length

As discussed in subsection 2.4.1, the sensing factor is a quantity which determines how strong the presence of a glass particle influences the optical properties of the cavity. Equation 2.8 is inversely proportional to the length of the cavity which was explained through the fact that a smaller mode volume will cause the volume of the nano-scaled, particle inside of the cavity to become larger in comparison to the mode volume. However, the cavity dimensions cannot be made arbitrarily small. At the minimum cavity length L , clipping losses of the trapping beam (see Figure 3.1) need to be negligible. Clipping of the trapping beam would dramatically reduce its efficiency and cause scattering of energy into undesired modes. It would also heat up the cavity mirror.

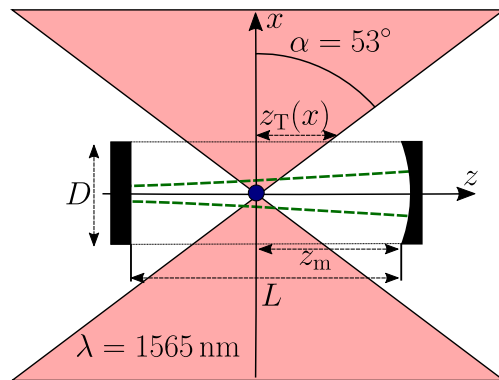


Figure 3.1: The figure shows a sketch of the trapping experiment. The green lines show the profile of the Gaussian mode. z_T is the radius of the trapping beam (red). The trapping beam has an NA of 0.8. z_m is the distance of the cavity mirror from the trapping beam's focus.

In the following discussion we will derive an analytical solution for the minimum cavity length given the trapping beams presence. Furthermore, the entire Gaussian mode cross section has to fit onto the mirror surface which dictates a minimum diameter D for the

3 Fabrication

mirrors. The problem ultimately boils down to minimizing L while at the same time maximizing D without intersecting with z_T .

To know the limit for the mirror diameter D we first need the trapping beam radius z_T . From Figure 3.1 we see that this radius can be described by the following formula:

$$z_T(x) = x \tan \alpha \quad (3.1)$$

Next we need to describe the mirror diameter D in relation to the Gaussian beam. The beam waist radius of a Gaussian beam is given by:

$$w(z) = w_0 \sqrt{1 + \left(\frac{z}{z_R}\right)^2} \quad (3.2)$$

where z_R is the Rayleigh length. The Rayleigh length is given by the beam waist radius at the focus of the Gaussian beam and by its wavelength. We can now use this to determine D . Since the beam further diverges while coupling light out of the cavity the thickness of the mirror also needs to be considered. The polymer layer which forms the mirror can be estimated to have a thickness of around 25 μm and the glass cover slip where the mirror is fixed upon has a thickness of around 160 μm . The resulting thickness of both materials is summarized in the term δ . The beam waist radius we are interested in is therefore $w(z_m + \delta)$. To get the diameter from the radius we normally would multiply by two. However, to make sure that the entire beam hits the mirror we use a factor $\rho = 5$ instead. The diameter is then defined by:

$$D(z_m) = \rho \cdot w(z_m + \delta) \quad (3.3)$$

Through simple algebra the mirror distance from the trapping beam focus is then given by:

$$z_m(D) = z_R \sqrt{\left(\frac{D}{\rho w_0}\right)^2 - 1 - \delta} \quad (3.4)$$

As stated at the beginning, we need to make D as large as possible while keeping z_m as small as possible. This requirement can be stated as follows:

$$2 \cdot z_T(x = D/2) = z_m(D) \quad (3.5)$$

Note that we put a factor two in front of the trapping beam radius for safety reasons. If we plug Equation 3.4 and Equation 3.1 into our requirement we get a quadratic equation which can be solved for D .

$$D = \frac{-\delta \tan \alpha + \sqrt{\delta^2 \tan^2 \alpha - \left[\tan^2 \alpha - \left(\frac{z_R}{\rho w_0}\right)^2\right] [\delta^2 + z_R^2]}}{\tan^2 \alpha - \left(\frac{z_R}{\rho w_0}\right)^2} \quad (3.6)$$

Now we can estimate the cavity length $L = 2 \cdot z_m(D) + \delta$. To get actual numbers we have to fix the beam waist radius w_0 of the cavity mode at the focus. The estimated value for w_0 can range from 2 μm to about 40 μm . In reality the focus width will be determined by the cavity dimensions themselves. To stay within the defined range of w_0 a cavity which has a length of $L \approx 500 \mu\text{m}$ with mirrors of diameter $D \approx 200 \mu\text{m}$ is a very robust choice.

3.1.2 Wavefront radius

For a Gaussian mode to resonate inside the cavity the wavefront radius of the beam has to match the curvature of the cavity mirror. Since we are using a hemispherical cavity, primarily for alignment reasons [ref], we have one mirror without curvature and one mirror which is spherical. The wavefront radius of the beam depends on the cavity length L .

$$R(L) = L \left[1 + \left(\frac{z_R}{L} \right)^2 \right] \quad (3.7)$$

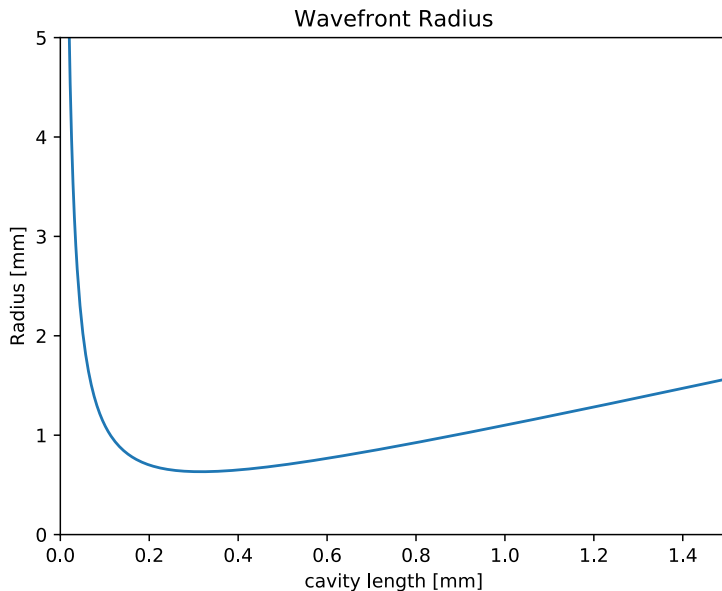


Figure 3.2: This figure shows the dependence of the wavefront radius R of the Gaussian beam on the cavity length L at a fixed w_0 .

Equation 3.7 does also depend on the Rayleigh length z_R .

$$z_R = \frac{\pi w_0^2}{\lambda} \quad (3.8)$$

While discussing the cavity length in the last section it was stated that the beam waist radius at the origin which also defines the wavefront radius through z_R , is determined by the cavity dimensions and has a certain allowed range. This is the reason why the R does not have to be exact but can vary between 0.7 mm to 1.0 mm. This is very important for process stability as we will see later on.

3.1.3 Surface roughness

The surface roughness of the cavity mirrors is of paramount importance while planning the fabrication of the microcavity mirrors. How the surface roughness influences the

3 Fabrication

cavity losses is described by the following simple formula [ref]:

$$L_{sc} = \left(\frac{4\pi\sigma_{sc}}{\lambda} \right)^2 \quad (3.9)$$

The finesse which defines what portion of the light remains inside of the cavity after one round trip is defined as [ref]:

$$\mathcal{F} = \frac{2\pi}{L_{sc}} \quad (3.10)$$

It can be seen that the finesse degrades substantially with an increasing surface roughness.

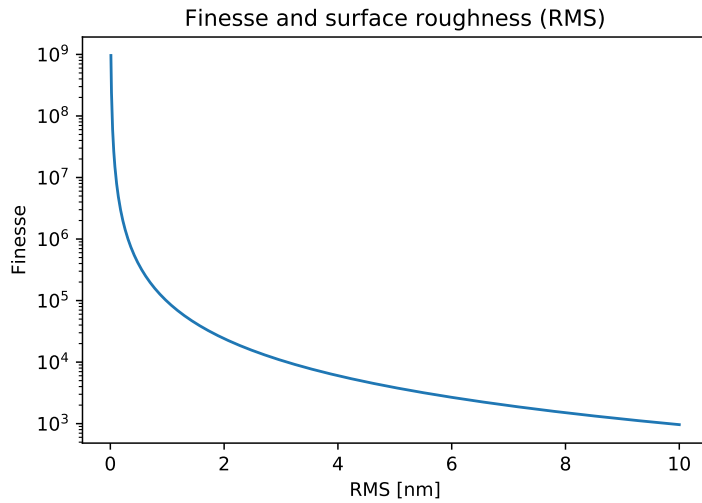


Figure 3.3: It can be seen how the finesse of the cavity degrades as a function of the surface roughness (RMS). From a roughness of 0.5nm to 1.5nm the finesse has already degraded by one order of magnitude.

As explained in subsection 2.4.2, the linewidth of the cavity has to be large enough such that the particle motion can be followed without much delay. This means the finesse cannot be too high. However, the lowering of the finesse has to take place through the light leaving the cavity through one of the mirrors and not through scattering losses due to rough mirror surfaces. For this reason the aim is to fabricate mirrors with a roughness below 0.6 nm which corresponds to a scattering loss of less than 23.4 ppm.

3.2 Process

In the following section the fabrication process that was put together, based on extensive research with different fabrication approaches, will be described in detail.

3.2.1 Overview

The fabrication of the microcavity consists mainly in the manufacturing of a tiny spherical mirror. Figure 3.4 shows schematically in what order the different steps of the fabrication process are arranged.

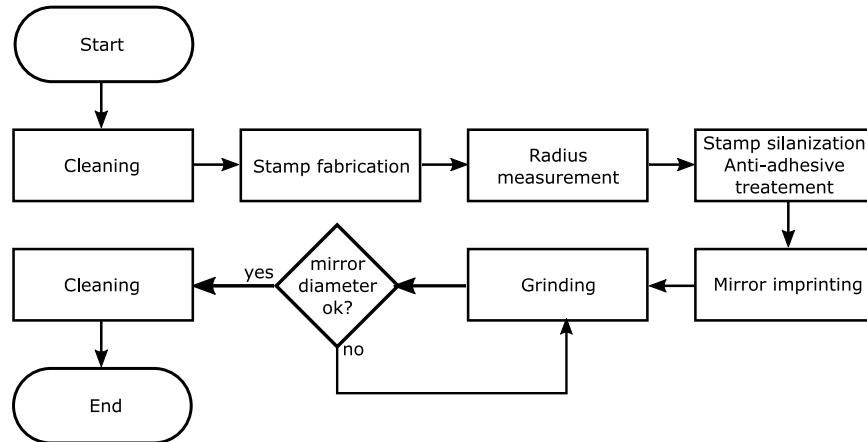


Figure 3.4: This flowchart shows schematically in which order the various fabrication steps are arranged.

The process produces in the end a transparent shape of the mirror. In order for the mirror to fulfill its purpose it has to be coated with a reflective layer. This step is done by [company], an external company that specializes in coating sensitive structures on different scales.

3.2.2 Cleaning

The complete fabrication process takes quite some time to be completed. All steps combined up to the point where the mirror shape can be measured to determine its surface roughness, takes about twenty hours. To protect the mirrors from being contaminated while being fabricated, all fixtures and tools have to be clean. They are cleaned by putting them into a bath of acetone and then ultrasonicate them for roughly twenty minutes. After that the step is repeated with Isopropanol (longname) instead of acetone. Drying the components in an oven finalizes this step.

3.2.3 Stamp fabrication

The fabrication of the stamps is one key step in the fabrication process. Fabricating the steps reliably is crucial to make the process stable. Various methods for creating stamps made from Siliciumdioxide exist. Some use pulsed lasers to melt them [ref]. Other

3 Fabrication

methods use cylindrical holes to let spherical drops form inside while the whole setup is put into a high temperature oven [ref]. Our method uses a small blowtorch [ref] which can be bought regularly and a specially made machine which spins the glass medium while it is being melted. With the spinning it is ensured that the drop that the glass forms a symmetrical, spherical drop while being melted.

The material we use for this procedure are glass cylinders extracted from a standard multimode communication fiber of one millimeter thickness. To do this we use a special tool is used to remove the cladding. After that, we ultrasonicated the fiber piece in Acetone to remove the buffer layer. With this done the melting procedure can be initiated.

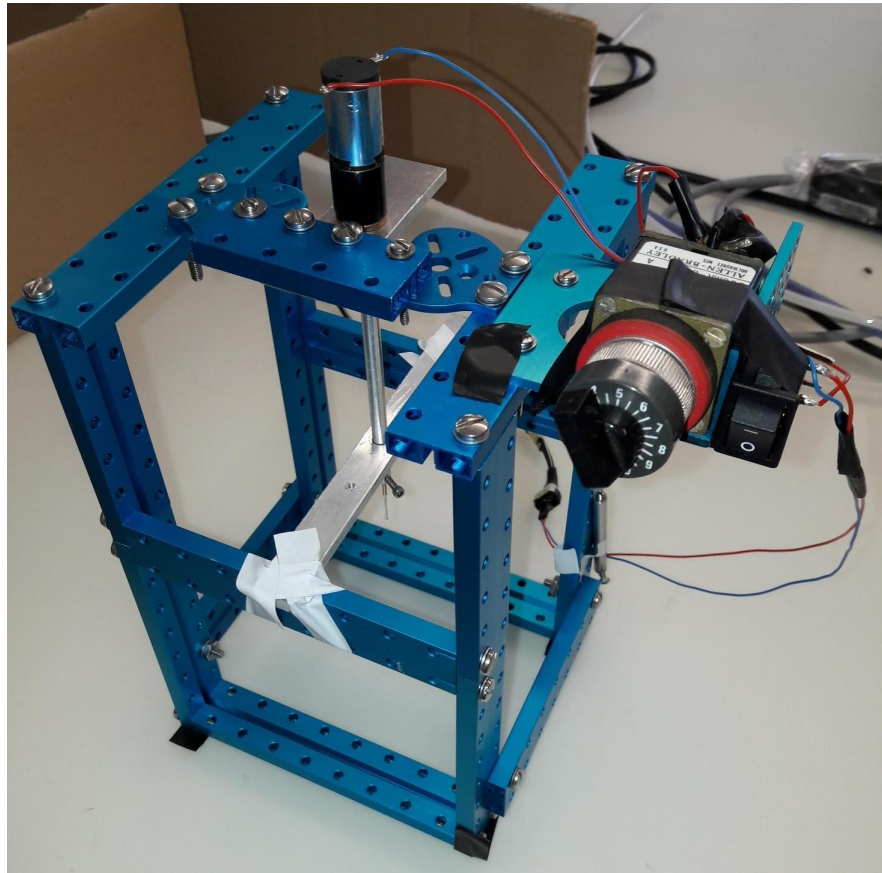


Figure 3.5: A picture of the machine used for melting the glass rods. The framing is made from a construction kit from Makeblock. Some parts of the framing are custom made parts made from aluminum. The motor is from Maxxon (870 rpm, 41Nmm).

Without the spinning at approximately 11.4Hz (would be around 14.5Hz without the straightening fixture around the axles) the drop would not form a sphere in a controlled manner. Figure 3.6 shows schematically how the formation without the spinning motion would look.

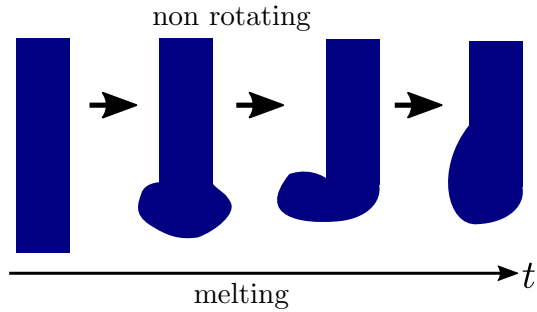


Figure 3.6: Schematic depiction of a drop melted without the rotating motion during the process.

With the machine shown in Figure 3.5 this problem can be omitted and the radius of the drop can be controlled by varying the speed of the machine and also by holding the blowtorch at different heights.

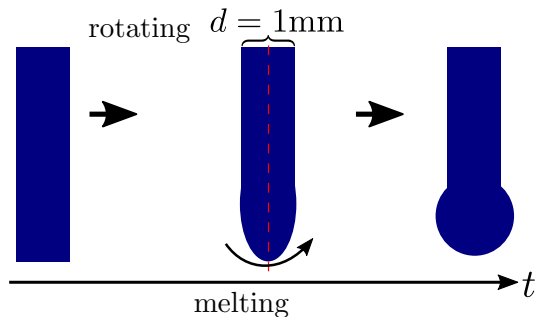


Figure 3.7: Schematic depiction of the melting process with rotating axis.

For the actual melting we used two different process gases: Acetylene at a pressure of 0.4bar and Oxygen at a pressure of 0.2bar. To prevent soot from contaminating the stamp it is important to add Oxygen to the Acetylene flame. If the yellow in the flame disappears and a blue glow is emitted from the center of the flame the blowtorch is set up properly. The melting then simply takes place by holding the flame of the blowtorch up to the rotating glass cylinder at approximately four millimetres above the lower end and waiting for the glass to melt and expand into a sphere. The blowtorch can then be turned off and in a short amount of time the glass cools down and forms a transparent sphere at the lower end of the cylinder.

3 Fabrication



Figure 3.8: In this picture it can be seen how the rotating glass rod forms a drop which is spherical in the front. After cooling the surface is smooth [ref] and the stamp can be further processed.

3.2.4 Measurement

After the stamps have been fabricated their respective sphere radii have to be determined. The most frontal part of the glass stamp will imprint the spherical mirror shape into the polymer. This means that the radius of the front part of the stamp has to be known. For this purpose the stamps are fixed inside a quartz-dish and photographed with a microscope. From this image a software developed in python can determine the radius of the spherical region that will be used as the actual stamp.

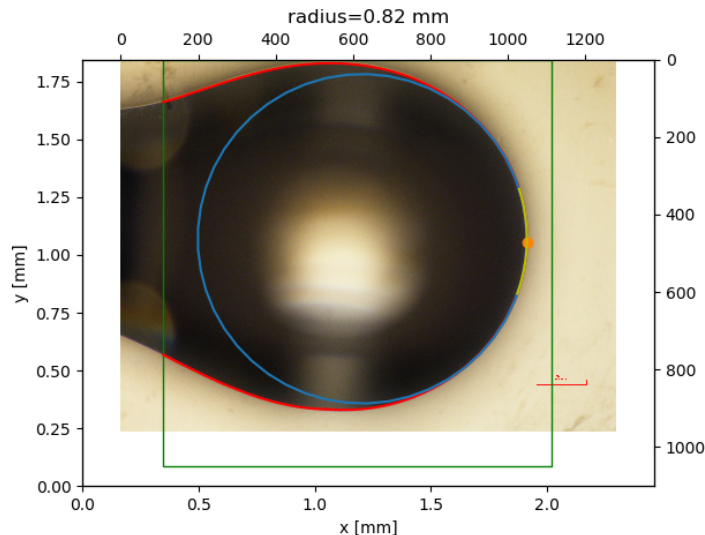


Figure 3.9: The software that is used for extracting the radius is developed in python. It is able to determine the orientation of a sample and uses this to predict which part of the stamp will be in contact with the polymer (marked yellow). The contact region is then used to extract the radius with at this position with the Ransac (Random sample consensus) [ref] algorithm.

The mean radius across the fabricated stamps is $797 \mu\text{m}$ with a standard deviation of

3.2 Process

59 µm. From the radius we can then infer the dimensions of the actual mirror. First we need the beam waist radius in the focus so we can calculate the Rayleigh range. The wavefront radius is now fixed since the stamp is already fabricated and the cavity length we choose to be 500µm as discussed in subsection 3.1.1. The following formula for the beam waist radius in the focus can be found by plugging Equation 3.8 into Equation 3.7:

$$w_0(R, L) = \sqrt{\frac{\lambda}{\pi}} (L(R - L))^{1/4} \quad (3.11)$$

We know from our discussion regarding the the cavity length that the mirror diameter D will be around 200 µm. Given that R, L and w_0 are known we can use Equation 3.3 to get a specific value for D . From this we can calculate the mirrors depth with simple, geometrical considerations:

$$h = R - \sqrt{R^2 - \left(\frac{D}{2}\right)^2} \quad (3.12)$$

The diameter of the mirrors surface that will actually be hit by the light can be calculated as follows:

$$d_{\text{Beam}} = 2R \cdot \arctan\left(\frac{w(L)}{R}\right) \quad (3.13)$$

Where L is the cavity length.

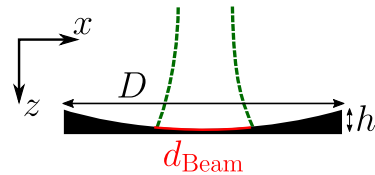


Figure 3.10: This sketch shows the different mirror dimensions quantities which can be estimated after the radius of the stamps has been determined.

The measured and the calculated quantities of the fabricated stamps have been summarized in Table 3.1.

3 Fabrication

Sample	R [μm]	Required w_0^* [μm]	d_{Beam}^* [μm]	D^* [μm]	h^* [μm]
1.1	890.6639	14.838	44.7991	136.8438	2.632
1.2	788.4094	13.7539	45.4682	141.8371	3.1961
1.3	817.886	14.0926	45.1984	140.0812	3.0045
1.4	750.304	13.2752	45.9537	144.6518	3.4941
1.5	744.3828	13.196	46.0465	145.1573	3.5467
1.6	898.1311	14.9084	44.7742	136.5796	2.6
1.7	718.6489	12.834	46.5184	147.6193	3.8004
1.8	884.216	14.7764	44.8226	137.0806	2.6605
1.9	769.0092	13.5166	45.6931	143.1823	3.3396
1.10	708.7698	12.6865	46.734	148.6966	3.9103
1.11	734.1915	13.0562	46.2193	146.0779	3.6421
2.1	797.1162	13.8566	45.3802	141.285	3.1364
2.2	789.5671	13.7677	45.4561	141.7619	3.188
2.3	856.5509	14.5029	44.9471	138.1972	2.7917
2.4	782.7343	13.6858	45.5297	142.2135	3.2365
3.1	813.2913	14.0414	45.2354	140.3347	3.0325

Table 3.1: The table shows the measured radii R alongside the calculated (*) values for the expected beam radius at the focus w_0 , the beam diameter on the mirror surface d_{Beam} the diameter of the mirror D and the depth of the mirror h .

3.2.5 Silanization

As imprinting medium we use a polymer called OrmoComp (made by the German company Microresist) [ref]. This polymer is made for imprinting small details and curing it afterwards with UV-light. To improve the quality of the imprints it is important to use an anti-adhesive agent which prohibits the polymer from sticking to the stamp after it has been hardened. Anti-adhesive agents are chemical compounds which belong to the Silane group, hence the term *silanization* [ref]. For our silanization we used a silane called *1H,1H,2H,2H-perfluorooctyl-trichlorosilane* (usually shortened to *F13-TCS*).



Figure 3.11: Left: Stamps fixed at the bottom of the quartz dish. Right: Setup used for silanization.

3.2 Process

Since F13-TCS reacts strongly with water it is important that the moisture in the environment is kept at a minimum during the silanization process. To achieve this, we taped our stamps to the bottom of a quartz dish, put them onto a hot plate and flushed them with a weak but steady stream of nitrogen (see Figure 3.11). The entire process takes place under flow hood (model). This procedure continues for thirty minutes while the quartz dish is heated to 50 °C.

After thirty minutes, the nitrogen flow is removed and a small amount (0.5 – 1.0 µl) of the F13-TCS is put next to the stamps without touching them. At 50 °C the silane will evaporate and ideally its molecules will bind to the surfaces of the stamps and build up an anti-adhesive monolayer [ref].

After an additional thirty minutes the hotplate is turned off. The quartz dish, remains closed and under the flow hood until it reaches room temperature.

There are process manuals which include a plasma treatment of the stamps upfront [ref]. In our process we have omitted this step since the stamps have been melted less than an hour prior to the silanization and should therefore still have active [insert good explanation].

3.2.6 Coverslip preparation

The polymer which was described in the last section is located on a glass coverslip which serves as a base for the mirror. To add the polymer layer to the coverslip we follow a specific procedure.

First, we get the pre-cleaned coverslip from a beaker where it was stored in DI water. The coverslip is then dried and put into a plasma chamber ([device]). To enhance the adhesion of the polymer to the glass a treatment with oxygen plasma is applied over a duration of approximately two minutes. The next step is to use a spin-coating machine ([device]) to create an even layer of the polymer. This process takes place in a yellow room since the polymerization of the OrmoComp polymer which we are using, starts very quickly when exposed to UV-light sources. The spin-coating takes thirty seconds and takes place at a rotational speed of 3000 rpm. The coated coverslip is then put onto a hotplate at 80 °C and left there for two minutes. This concludes the coating and pre-baking, the polymer layer has now a thickness of 20 – 25 µm [ref] and can be used for imprinting.

3.2.7 Mirror imprinting

3.2.8 Grinding

3.2.9 Cleaning

3.2.10 Coating

Our lab is not equipped with the tools necessary to add a well defined reflective coating to smooth surfaces. This is why the nearly finished cavity mirrors are sent in for coating at [company]. [Describe the process]

3 Fabrication

3.3 Process Evaluation

The process described in the last section was the result of many hours of research and experiments. This section will discuss the different approaches which were taken to implement this process. Furthermore, we will discuss why certain approaches were chosen over their alternatives and what the problems of those approaches are.

3.4 Analysis

4 Results

5 Summary and Outlook

The goal of this work was to design and build a narrow linewidth $\kappa < 2\pi \times 10 \text{ kHz}$ optical cavity able to resolve the motional sidebands of an optically levitated nanosphere. Furthermore, the cavity resonance needed be stable enough to allow to lock a laser to the cavity in a stable manner.

During the design process, particular attention was put on obtaining a cavity with a stable resonance frequency, by minimizing the influence of environmental disturbances (in particular thermal and mechanical noise) to the cavity resonance. To this end, in the cavity construction, materials with low thermal expansion rates were employed and an active stabilization of the cavity temperature was implemented. Furthermore, a vibration isolation system as well as a vacuum setup were built.

A laser was successfully frequency locked to the cavity using the Pound-Drever-Hall locking technique. The laser was stabilized to the cavity resonance more precisely than κ and the lock remained stable against perturbations (knocking on the optic table, clapping), proving that the isolation of the cavity from environmental mechanical and acoustic noise was efficient enough. To this point it was not possible to quantitatively characterize the stability of the cavity resonance with respect to temperature fluctuations in the environment, i.e. determine the coefficient of thermal expansion of the mirror spacer. As soon as a stable (absolute) frequency source is available this value will become accessible. Being able to stabilize the laser to the cavity was a first step towards a frequency locked system consisting of microcavity, external cavity and optical field (Fig. ??).

Finally, important parameters characterizing the cavity were determined. Among them, the cavity linewidth was found to be $\kappa \approx 2\pi \times 40.34(4) \text{ kHz}$, a larger value than the linewidth that was computed based on the mirror specifications. Consistently, the absorption in the cavity mirrors was measured to be higher ($\mathcal{A} \approx 122(6) \text{ ppm}$) than expected ($\mathcal{A} < 1 \text{ ppm}$). Determining the reasons for the increased absorption \mathcal{A} remains a task for the future.

Acknowledgements

I would like to thank Prof. Dr. Lukas Novotny, Dominik Windey and Dr. René Reimann for the opportunity of working on this semester thesis.

During the entire project I could always rely on the supervision of either Dominik Windey or Dr. René Reimann if questions of any sort arose. Their knowledge and the time they took to explain the principles of cavity dynamics in the context of this thesis was very much appreciated. Furthermore, I like to thank them for reading this report and being upfront and honest with their criticism, which helped to greatly improve the quality of this work.

Many thanks go to Anna Kuzmina. Her help was not only appreciated but also crucial to many insights that were gained during the course of this work. The many hours which she spent assisting my project were invaluable. She was always patient and precise while helping and also during the many discussions which we had.

Furthermore, I also want to say a special "thank you" to Dr. Martin Frimmer for the many instances where he made suggestions and the many times he gave valuable tips regarding this work.

Additionally, I want to thank Dr. Achint Jain, who assisted me greatly with the AFM measurements and the evaluation of the data, even though he also had to prepare his PhD defense.

Finally, I want to thank every member of the Photonics Laboratory, for all the interesting discussions, the help and the generally friendly, open and inclusive environment I had the privilege to work in.